# Synthesis and Structures of New Layered Ternary Manganese Tellurides: $AMnTe_2$ (A = K, Rb, Cs), $Na_3Mn_4Te_6$, and $NaMn_{1.56}Te_2$

**Joonyeong Kim, Chwanchin Wang,† and Timothy Hughbanks***

Department of Chemistry, Texas A&M University, P.O. Box 30012, College Station, Texas 77842-3012

*Received July 15, 1998*

The synthesis and crystal structures of new ternary manganese tellurides, $AMnTe_2$ (A = K, Rb, Cs), $Na_3Mn_4Te_6$, and $NaMn_{1.56}Te_2$, are reported. These compounds are synthesized by solid-state reaction and cation exchange techniques in sealed Nb tubes. The single-crystal structures of $AMnTe_2$ (A = K, Rb), $Na_3Mn_4Te_6$, and $NaMn_{1.56}Te_2$ have been determined; $KMnTe_2$: $a = 4.5110(4)$ Å, $c = 14.909(2)$ Å, $I\bar{4}m2$ (No. 119, $Z = 2$); $RbMnTe_2$: $a = 4.539(1)$ Å, $c = 15.055(2)$ Å, $I\bar{4}m2$ (No. 119, $Z = 2$); $Na_3Mn_4Te_6$: $a = 8.274(4)$ Å, $b = 14.083(6)$ Å, $c = 7.608(6)$ Å, $\beta = 91.97(4)°$, $C2/m$ (No. 12, $Z = 2$); $NaMn_{1.56}Te_2$: $a = 4.4973(8)$ Å, $c = 7.638(2)$ Å, $P\bar{3}m1$ (No. 164, $Z = 1$). The fundamental building blocks of the title compounds are $MnTe_4$ tetrahedra. $AMnTe_2$ (A = K, Rb, Cs) are isostructural with $TlFeS_2$, consisting of layers built up by four corner-shared $MnTe_4$ tetrahedra. Manganese telluride layers in $Na_3Mn_4Te_6$ consist of two hexagonal nets of Te atoms between which two-thirds of the tetrahedral interstices are filled with Mn atoms to form two $6^3$ honeycomb nets. $NaMn_{1.56}Te_2$ adopts a defective $CaAl_2Si_2$ structure type, in which Mn atoms partially and randomly occupy 78% of tetrahedral sites. Temperature-dependent magnetic susceptibilities measurements show that $AMnTe_2$ (A = K, Rb, Cs) exhibit Curie−Weiss paramagnetism, whereas $Na_3Mn_4Te_6$ and $NaMn_{1.56}Te_2$ show paramagnetism with a weak dependence on temperature.

## Introduction

There is much current interest in ternary systems with A−M−Q compositions (A = alkali metals; M = Mn, Fe, Co, Ni; Q = chalcogen). This has led to the synthesis of many new materials with unusual structural features and physical properties that deserve further investigation.[1−17] Most investigations of such A−M−Q ternary systems have concentrated on sulfides and selenides; with less attention paid to tellurides. Some notable exceptions to this generalization include contributions by Bronger and Klepp.[1,4,15,16,18]

Our interest in layered ternary manganese tellurides was sparked by the serendipitous discovery of the polar layered compounds, $LiMnTe_2$ and $NaMnTe_2$.[19] We believe that layered compounds with intrinsic polarity to be interesting potential hosts for composite materials prepared by intercalation of nonlinear optical chromophores.[20,21] In these compounds, there also exists the possibility that interesting magnetic properties might accompany such behavior. Bronger and co-workers reported the only other ternary manganese tellurides known, all of which fall into three types: $A_2MnTe_2$ (A = K, Rb, Cs), $A_6MnTe_4$ (A = Na, K), and $A_2Mn_3Te_4$ (A = Rb, Cs).[4,15,16] In the first of these structure classes, one-dimensional chains, ${}^1_\infty[MnTe_2]^{2-}$, built up by edge-sharing of $MnTe_4$ tetrahedra are found. Discrete $[MnTe_4]^{6-}$ tetrahedra are found in the second structure class. The third series of compounds possess layered structures, ${}^2_\infty[Mn_3Te_4]^{2-}$, as will more fully described below. We have uncovered several new layered compounds, $AMnTe_2$ (A = K, Rb, Cs), $Na_3Mn_4Te_6$, and $NaMn_{1.56}Te_2$ and this paper report the synthesis and structures of these new compounds. We also discuss structural relationships between the title compounds and other related compounds. A preliminary communication of some of this work has been published.[19]

* To whom correspondence should be addressed.

† Present address : Department of Chemistry, Princeton University, Princeton, NJ 08544.

(1) Klepp, K. O.; Sparlinek, W.; Boller, H. *J. Alloys Compd.* **1996**, *238*, 1−5.
(2) Huan, G.; Greenblatt, M.; Croft, M. *Eur. J. Solid State Inorg. Chem.* **1989**, *26*, 193−220.
(3) Bronger, W.; Rennau, R. M.; Schmitz, D. *Z. Anorg. Allg. Chem.* **1996**, *622*, 627−629.
(4) Bronger, W.; Hardtdegen, H.; Kanert, M.; Schmitz, D. *Z. Anorg. Allg. Chem.* **1996**, *622*, 313−318.
(5) Bronger, W.; Koelman, W.; Schmitz, D. *Z. Anorg. Allg. Chem.* **1995**, *621*, 405−408.
(6) Bronger, W.; Bomba, C.; Koelman, W. *Z. Anorg. Allg. Chem.* **1995**, *621*, 409−411.
(7) Bronger, W.; Muller, P. *Z. Anorg. Allg. Chem.* **1995**, *621*, 412−416.
(8) Bronger, W.; Ruschewitz, U.; Müller, P. *J. Alloys Compd.* **1995**, *218*, 22−27.
(9) Bronger, W.; Balk-Hardtdegen, H.; Ruschewitz, U. *Z. Anorg. Allg. Chem.* **1992**, *616*, 14−18.
(10) Bronger, W.; Ruschewitz, U.; Müller, P. *J. Alloys Compd.* 1992, *187*, 95−103.
(11) Bronger, W.; Rennau, R.; Schmitz, D. *Z. Anorg. Allg. Chem.* **1991**, *597*, 27−32.
(12) Bronger, W.; Kyas, A.; Müller, P. *J. Solid State Chem.* **1987**, *70*, 262−270.
(13) Bronger, W.; Schmitz, D. *Z. Kristallogr.* **1988**, *183*, 201−205.
(14) Bronger, W.; Hendriks, U.; Müller, P. *Z. Anorg. Allg. Chem.* **1988**, *559*, 95−105.
(15) Bronger, W.; Balk-Hardtdegen, H. *Z. Anorg. Allg. Chem.* **1989**, *574*, 89−98.
(16) Bronger, W.; Balk-Hardtdegen, H.; Schmitz, D. *Z. Anorg. Allg. Chem.* **1989**, *574*, 99−106.
(17) Bronger, W.; Bomba, C. *J. Less-Common Met.* **1990**, *158*, 169−176.
(18) Bronger, W.; Bonsmann, B. *Z. Anorg. Allg. Chem.* **1995**, *621*, 2083−2088.
(19) Kim, J.; Wang, C.; Hughbanks, T. *Inorg. Chem.* **1998**, *37*, 1428−1429.
(20) Lacroix, P. G.; Clément, R.; Nakatani, K.; Zyss, J.; Ledoux, I. *Science* **1994**, *263*, 658−660.
(21) Lagadic, I.; Lacroix, P. G.; Clément, R. *Chem. Mater.* **1997**, *9*, 2004−2012.

10.1021/ic980805w CCC: $18.00 
Published on Web 12/30/1998

## Experimental Section

**Materials and Instrumentation.** As the compounds described herein are sensitive to both moisture and oxygen, experimental operations were carried out under an inert gas atmosphere. Elemental starting materials were Mn (99.99%, Johnson Matthey), Te (99.997% Aldrich), Li (99.0%, Aldrich), Na (99.0%, Aldrich), and K (99.0%, Aldrich). LiCl (>99.0%, Aldrich), KCl (>99.0%, Aldrich), RbCl (>99.0%, Aldrich), and CsCl (>99.0%, Aldrich) were sublimed at least twice before use. $Li_2Te$, $Na_2Te$, and $K_2Te$ were synthesized in liquid $NH_3$ as described in the literature[22,23] and purity was confirmed by examination of Guinier X-ray powder patterns. $LiMnTe_2$ was prepared by loading a 1:1:2 ratio of Li/Mn/Te in a sealed Nb tube which was in turn sealed in an evacuated ($\sim 10^{-4}$ Torr) and flame-baked silica tube as described in a previous communication;[19] its identity was confirmed by measuring the Guinier X-ray powder pattern before use. All compounds were synthesized by the use of Nb tubes that were in turn sealed in an evacuated ($\sim 10^{-4}$ Torr) silica tube. Atomic absorption (AA) measurements were performed on a Varian SpectrAA 250 Plus instrument after dissolution of products in 20% (w/w) nitric acid. Standard solutions for AA measurements are purchased from Aldrich. For each element, measurements on at least three standard solutions were taken with different concentrations to obtain a linear calibration plot. Wavelength-dispersive X-ray spectrometry (WDS) analyses were performed using a Cameca SX 50 scanning electron microscope. Samples for AA and WDS measurements were gathered by selecting crystals from the reaction products.

Temperature-dependent magnetic susceptibilities were measured with a LakeShore 7229 AC susceptometer with an external field strength 10 Oe over the temperature range 4−300 K for selected crystals of title compounds. Data were corrected for the diamagnetic contributions of the atomic cores[24] and sample holder.

**Synthesis.** $AMnTe_2$ (A = K, Rb, Cs) compounds were synthesized by mixing $LiMnTe_2$, LiCl, and ACl (A = K, Rb, Cs) in 1:2:2 mole ratios in a sealed Nb tube. In each case, the temperature was uniformly raised from room temperature to 750 °C over 4 days, held at that temperature for 200 h, and finally cooled to room temperature at a rate of 2 °C/h. All products contained dark-red single crystals suitable for X-ray crystallography. Excess ACl (A = K, Rb, Cs) and LiCl were removed from the desired products by washing with dried methanol under a nitrogen atmosphere. Microprobe analysis on selected crystals showed the compositions $K_{0.93(1)}Mn_{1.09(3)}Te_2$, $Rb_{0.91(1)}Mn_{1.05(1)}Te_2$, and $Cs_{0.88(1)}Mn_{1.04(1)}Te_2$. No other elements heavier than Na were found. Atomic absorption analyses were carried out to independently determine compositions and yielded the following results: $K_{0.97(1)}Mn_{1.08(3)}Te_2$, $Rb_{0.98(1)}Mn_{1.01(1)}Te_2$, and $Cs_{1.00(1)}Mn_{0.94(1)}Te_2$. AA measurements showed no detectable Li in these compounds.

$Na_3Mn_4Te_6$ and $NaMn_{1.56}Te_2$ were first found in our attempts to synthesize $NaMnTe_2$ directly from the elemental starting materials.[19] A reaction loaded using elemental sodium, manganese, and tellurium combined in a 3:4:6 ratio was conducted in a sealed Nb capsule which was in turn sealed in an evacuated ($\sim 10^{-4}$ Torr) and flame-baked silica tube. The temperature of the reaction vessel was uniformly raised to 450 °C over 2 days, maintained at 450 °C for 2 days, uniformly increased to 600 °C for 2 days, and then maintained at that temperature for 1 week. It was then cooled to room temperature at a rate of 1 °C/h. Red crystals of $Na_3Mn_4Te_6$ suitable for X-ray crystallography were found. $NaMn_{1.56}Te_2$ was synthesized by mixing elemental Na, Mn, and Te in stoichiometric proportions in Nb tubes. The temperature of reaction vessel was uniformly raised to 450 °C for 2 days, maintained at 450 °C for 2 days, uniformly increased to 850 °C over 3 days, held at that temperature for 200 h, and finally cooled to room temperature at a rate of 2 °C/h. Dark-red platelike crystals suitable for X-ray studies were found. Microprobe analysis on selected crystals from the products of both $Na_3Mn_4Te_6$ and $NaMn_{1.56}Te_2$ showed approximate compositions $Na_{2.90(3)}Mn_{3.95(2)}Te_6$ and $Na_{1.01(1)}Mn_{1.54(1)}Te_2$, respectively. No other elements heavier than Na, including Nb, were found in either case. Atomic absorption measurements for both compounds gave the respective compositions $Na_{2.91(2)}Mn_{4.02(1)}Te_6$ and $Na_{0.99(1)}Mn_{1.57(1)}Te_2$.

**X-ray Crystallography.** X-ray diffraction data of $KMnTe_2$, $RbMnTe_2$, $Na_3Mn_4Te_6$, and $NaMn_{1.56}Te_2$ were collected on a Siemens R3m/V diffractometer with graphite-monochromated Mo Kα radiation ($\lambda = 0.710\ 73$ Å) at 20 °C. Structure refinements of these compounds were based on $F^2$ with the use of the SHELX-93 package of programs.[25]

A dark-red platelike crystal of $KMnTe_2$ having approximate dimensions 0.12 × 0.10 × 0.03 mm was mounted in a glass capillary. Tetragonal cell constants and an orientation matrix were obtained from a least-squares refinement using the setting angles from 15 centered reflections. This cell was refined by centering on 24 reflections in the range $15 \le 2\theta \le 35°$. Intensity data were collected by use of $\theta-2\theta$ scans for reflections with $2\theta < 60°$. Three check reflections monitored every 97 reflections throughout the data collection process showed no significant trends. A hemisphere of the data was collected ($+h, \pm k, \pm l$) to gain the advantage of averaging. The data were corrected for absorption using the $\psi$ scan technique based on five reflections. 166 reflections were unique, and 158 reflections with $I > 2\sigma(I)$ were used in the refinements. Systematic absences ($h + k + l = 2n + 1$), Guinier X-ray diffraction data, and elemental analysis suggested that $KMnTe_2$ is isostructural with the known phase $TlFeS_2$, with tetragonal space group $I\bar{4}m2$, so the atomic positions of $TlFeS_2$ were used to begin refinement of the $KMnTe_2$ structure.[26] Isotropic refinement of the structure with all K, Mn, and Te positions fully occupied resulted in a residual ($R$) of 6.96%. Final anisotropic refinement of $KMnTe_2$ gave 4.86 and 10.34% for final R($F$) and wR2($F^2$) with $I > 2\sigma(I)$. The largest remaining peaks in the final Fourier difference map were 1.265 e/Å$^3$ located close to Te in the framework of the structure.

A dark-red platelike crystal of $RbMnTe_2$ with approximate dimensions 0.08 × 0.08 × 0.04 mm was selected and mounted in a glass capillary. Preliminary Guinier X-ray powder patterns were used to establish tetragonal unit cells and to obtain lattice parameters. Cell constants and an orientation matrix were obtained from a least-squares refinement using 24 centered reflections in the range of $15 \le 2\theta \le 35°$. Intensity data were collected in the $\theta-2\theta$ scanning mode for reflections with $5 \le 2\theta \le 50°$. A hemisphere ($+h, \pm k, \pm l$) of data was collected. Three check reflections were monitored periodically and showed no significant change during the data collection process. The data set was corrected for absorption using the $\psi$ scan technique based on five reflections. All data except those for which $h + k + l = 2n + 1$ were observed, consistent with a body centered tetragonal space group. 109 reflections were unique, and 105 reflections with $I > 2\sigma(I)$ were used in the refinements. $RbMnTe_2$ is isostructural with $KMnTe_2$ so the atomic positions of $KMnTe_2$ were used to begin refinement of the $RbMnTe_2$ structure. Isotropic refinement of $RbMnTe_2$ showed reasonable thermal coefficients for all atoms. Final anisotropic refinement of $RbMnTe_2$ gave 4.07 and 9.25% for final R($F$) and wR2($F^2$) with $I > 2\sigma(I)$. The largest residual peak in the final Fourier difference map was 1.395 e/Å$^3$ located close to Te in the framework of the structure.

Elemental analyses and Guinier X-ray powder diffraction patterns of $CsMnTe_2$ showed that it is isostructural with $AMnTe_2$ (A = K, Rb). Cell parameters of $CsMnTe_2$ were refined by use of Guinier X-ray powder patterns. Cell parameters and volumes of $AMnTe_2$ (A = K, Rb, Cs) are listed in Table 1.

A red platelike crystal of $Na_3Mn_4Te_6$ with approximate dimensions 0.16 × 0.10 × 0.02 mm was selected and mounted in a glass capillary. Indexing of Guinier X-ray powder patterns had established a monoclinic unit cell and lattice parameters. Monoclinic cell constants and an orientation matrix were also obtained from a least-squares refinement using 24 centered reflections in the range of $15 \le 2\theta \le 35°$. Intensity data were collected in the $\theta-2\theta$ scanning mode for reflections with $5 \le 2\theta \le 50°$. Data were collected over one quadrant ($\pm h, +k, +l$).

(22) Feher, F. In *Handbuch der Preparativen Anorganischen Chemie*; Brauer, G., Ed.; Ferdinand Enke Verlag: Stuttgart, Germany, 1954.
(23) Klemm, W.; Sodomann, H.; Langmesser, P. *Z. Anorg. Allg. Chem.* **1939**, *241*, 281.
(24) Mulay, L. N., Boudreaux, E. A., Eds. *Theory and Application of Molecular Diamagnetism*; Wiley-Interscience: New York, 1976.
(25) (a) Sheldrick, G. M. *SHELXTL-93 User Guide*; Crystallography Department: University of Göttingen, Germany, 1993. (b) *SHELXTL-93 User Guide*, version 3.4; Nicolet Analytical X-ray Instruments: Göttingen, Germany, 1993.
(26) Kutoglu, A. *Naturwissenschaften* **1974**, *61*, 125−126.

**Table 1.** Lattice Parameters (Å)[a] and Cell Volumes (Å$^3$) of $AMnTe_2$ (A = K, Rb, Cs) with $TlFeS_2$ Structure Type Compounds with a Space Group *I*4*m*2

| | $KMnTe_2$ | $RbMnTe_2$ | $CsMnTe_2$ |
|---|---|---|---|
| *a* (Å) | 4.5110(4) | 4.539(1) | 4.5711(4) |
| *c* (Å) | 14.909(2) | 15.055(2) | 15.527(2) |
| *V* (Å$^3$) | 303.39(6) | 310.17(11) | 324.44(6) |
| *c*/*a* | 3.305 | 3.317 | 3.397 |

[a] Lattice parameters refined from Guinier powder diffraction patterns using Si as an internal standard.

Three check reflections every 97 reflections were monitored and showed no significant change during the data collection process. The data set was corrected for absorption using the $\psi$ scan technique based on five reflections. All reflections except those for which $h + k = 2n$ were absent, consistent with C-centering. An initial structural model for refinement of $Na_3Mn_4Te_6$ was found by direct methods. 567 reflections were unique, and 480 reflections with $I > 2\sigma(I)$ were used in the refinements. Isotropic refinement of $Na_3Mn_4Te_6$ showed reasonable thermal coefficients for all atoms. Anisotropic refinement of $Na_3Mn_4Te_6$ showed reasonable thermal parameters and gave 5.41 and 11.01% for final R(*F*) and wR2($F^2$) with $I > 2\sigma(I)$. The largest remaining peaks in the final Fourier difference map were 1.740 e/Å$^3$ close to a Mn atom in the framework of the structure.

A dark-red platelike crystal of $NaMn_{1.56}Te_2$ with approximate dimensions 0.20 × 0.18 × 0.06 mm was selected and mounted in a glass capillary. Indexing of Guinier X-ray powder patterns enabled us to establish the hexagonal unit cell and to obtain lattice parameters. Cell constants and an orientation matrix were obtained from a least-squares refinement using 24 centered reflections in the range of $15 \leq 2\theta \leq 35°$. Intensity data were collected in the $\theta-2\theta$ scanning mode for reflections with $5 \leq 2\theta \leq 50°$. Data ranging over the indices ($+h$, $+k$, $\pm l$) were collected. Three check reflections every 97 reflections were monitored periodically and showed no significant change during the data collection process. The data set was corrected for absorption using the $\psi$ scan technique based on five reflections. 111 reflections were unique and used in the refinements. No systematic absences were observed. An initial structural model for refinement of $NaMn_{1.56}Te_2$ was found by direct methods. Isotropic refinement of the structure with all Na, Mn, and Te positions fully occupied (corresponding to a "$NaMn_2Te_2$" composition) resulted in a residual (*R*) of 6.17%. However, the thermal parameter of Mn ($U_{iso} = 0.053$) was about 2 times larger than that of Te ($U_{iso} = 0.027$). When the thermal parameter of the Mn was fixed to be same as the Te atom, the refinement of the Mn site occupancy factor yielded 0.76(1) with a residual $R = 4.64\%$. This result was comparable to the composition obtained from WDS and AA measurements. In subsequent refinement cycles, both site occupancy and temperature parameters of Mn were refined simultaneously, which yielded in reasonable isotropic thermal parameters and a fractional site occupancy of 0.78(1). In the last cycle, the site occupancy of Mn was fixed and structure was refined anisotropically to yield respective residuals of 4.35 and 6.03% for final R(*F*) and wR2($F^2$) with $I > 2\sigma(I)$. The largest remaining peak in the final Fourier difference map was 1.405 e/Å$^3$ located near Te in the framework of the structure.

A summary of crystal and data collection parameters of $KMnTe_2$, $RbMnTe_2$, $Na_3Mn_4Te_6$, and $NaMn_{1.56}Te_2$ are listed in Table 2, and final atomic coordinates are shown in Table 3.

## Results and Discussion

**Syntheses.** Recently, new ternary manganese tellurides, $AMnTe_2$ (A = Li, Na), were discovered in our laboratories.[19] As these new compounds have unusual polar layers, $^2_\infty[MnTeTe_{3/3}]^-$, we investigated the possibility that corresponding $AMnTe_2$ (A = K, Rb, Cs) would adopt the same structure type. However, these compounds proved to be isostructural with $TlFeS_2$.

$AMnTe_2$ (A = K, Rb, Cs) can be synthesized at temperatures as low as 450 °C by reaction of $LiMnTe_2$ with a LiCl/ACl (A = K, Rb, Cs) flux, but the quality of crystals obtained from lower temperature reactions was not adequate for X-ray studies. Well-developed crystals of these compounds are obtained when the reaction temperature is 750 °C and cooling speed is slow (2 °C/h). Huan et al. used this method to synthesize ternary transition metal chalcogenides, $AM_2Q_2$ (A = Rb, Cs; M = Ni, Co; Q = S, Se), from the corresponding Tl compounds, $TlM_2Q_2$ (M = Ni, Co; Q = S, Se).[2] Attempts to synthesize $KMnTe_2$ by loading either elements or $K_2Te$, Mn, and Te as starting materials in stoichiometric proportions at 750 °C resulted in the formation of a mixture of $K_2MnTe_2$ and $KMnTe_2$. To optimize synthetic conditions for the synthesis of $KMnTe_2$, several reactions were attempted in which parameters such as loading composition, reaction time, temperature, and cooling speed were varied; in each case, a mixture of $K_2MnTe_2$ and $KMnTe_2$ was obtained. $KMnTe_2$ was generally found as a minor product. It appears that $KMnTe_2$ is a thermodynamically stable phase in the 450−800 °C temperature range, but that $K_2MnTe_2$, once formed, is unreactive and equilibrium is not attained in direct reactions. As the colors of $K_2MnTe_2$ and $KMnTe_2$ are similar (dark-red), it is impossible to physically separate $KMnTe_2$ from a reaction

**Table 2.** Crystallographic Data for $KMnTe_2$, $RbMnTe_2$, $Na_3Mn_4Te_6$, and $NaMn_{1.56}Te_2$

| chemical formula | $KMnTe_2$ | $RbMnTe_2$ | $Na_3Mn_4Te_6$ | $NaMn_{1.56}Te_2$ |
|---|---|---|---|---|
| *a*, Å | 4.5110(4) | 4.539(1) | 8.274(4) | 4.4973(8) |
| *b*, Å | | | 14.083(6) | |
| *c*, Å | 14.909(2) | 15.055(2) | 7.608(6) | 7.638(2) |
| *β*, deg | | | 91.97(4) | |
| *V*, Å$^3$ | 303.39(6) | 310.17(11) | 886.0(9) | 133.77(5) |
| *Z* | 2 | 2 | 2 | 1 |
| fw | 349.24 | 395.61 | 1054.33 | 363.90 |
| space group | *I*$\bar{4}$*m*2 (No. 119) | *I*$\bar{4}$*m*2 (No. 119) | *C*2/*m* (No. 12) | *P*$\bar{3}$*m*1 (No. 164) |
| *T* (°C) | 20 | 20 | 20 | 20 |
| *λ* (Å) | 0.710 73 | 0.710 73 | 0.710 73 | 0.710 73 |
| $\rho_{calcd}$ (g/cm$^3$) | 3.823 | 4.236 | 3.952 | 4.517 |
| $\mu$ (mm$^{-1}$) | 12.123 | 18.983 | 12.503 | 14.314 |
| R1[a] (%) | 4.86 | 4.07 | 5.41 | 4.35 |
| wR2[b](%) | 10.34 | 9.25 | 11.01 | 6.03 |

[a] $R1(F) = \sum(||F_o| - |F_c||)/\sum(|F_o|)$. [b] $wR2(F^2) = [\sum|w(F_o^2 - F_c^2)^2|/\sum|w(F_o^2)^2|]^{1/2}$, $w = 1/[\sigma^2(F_o^2) + (xP)^2 + yP]$, where $P = (\mathrm{Max}(F_o^2,0) + 2F_c^2)/3$.

**Table 3.** Atomic Coordinates and Equivalent Isotropic Displacement Parameters

| atom | position | *x*/*a* | *y*/*b* | *z*/*c* | $U_{eq}$[a] (Å$^2$ × 10$^3$) |
|---|---|---|---|---|---|
| | | | $KMnTe_2$ | | |
| K | 2*a* | 0.0 | 0.0 | 0.0 | 42(2) |
| Mn | 2*c* | 0.0 | 1/2 | 1/4 | 25(1) |
| Te | 4*e* | 0.0 | 0.0 | 0.3592(1) | 22(1) |
| | | | $RbMnTe_2$ | | |
| Rb | 2*a* | 0.0 | 0.0 | 0.0 | 27(1) |
| Mn | 2*c* | 0.0 | 1/2 | 1/4 | 11(2) |
| Te | 4*e* | 0.0 | 0.0 | 0.3563(1) | 16(1) |
| | | | $Na_3Mn_4Te_6$ | | |
| Na1 | 4*g* | 0.0 | 0.3422(16) | 0.0 | 68(9) |
| Na2 | 2*a* | 0.0 | 0.0 | 0.0 | 58(11) |
| Mn | 8*j* | 0.1668(8) | 0.1646(3) | 0.6279(7) | 35(2) |
| Te1 | 4*i* | 0.3022(5) | 0.0 | 0.7673(6) | 42(1) |
| Te2 | 8*j* | 0.1524(4) | 0.1763(2) | 0.2612(3) | 35(1) |
| | | | $NaMn_{1.56}Te_2$ | | |
| Na | 1*b* | 0.0 | 0.0 | 1/2 | 55(6) |
| Mn[b] | 2*d* | 2/3 | 1/3 | 0.8753(8) | 31(2) |
| Te | 2*d* | 2/3 | 1/3 | 0.2429(4) | 31(1) |

[a] Equivalent isotropic *U* defined as one-third of the trace of the orthogonalized $\mathbf{U}_{ij}$ tensor. [b] Occupancy 0.783(3).

mixture. The indirect cation exchange method described above proves to be the best means of obtaining $KMnTe_2$.

$Na_3Mn_4Te_6$ and $NaMn_{1.56}Te_2$ can be synthesized directly from elemental starting materials in sealed Nb tubes. $Na_3Mn_4Te_6$ and $NaMn_{1.56}Te_2$ were originally discovered in a reaction designed to directly synthesize $NaMnTe_2$.[19] A mixture of Na, Mn, and Te in a 1:1:2 ratio was loaded into a Nb reaction vessel that was in turn sealed in an evacuated ($\sim 10^{-4}$ Torr) and flame-baked silica tube. The temperature of the reaction vessel was uniformly raised to 450 °C for 2 days, maintained at that temperature for 2 days, uniformly increased to 600 °C for 2 days, held at that temperature for 1 week, and finally cooled to room temperature at a rate of 2 °C/h. Powder diffraction data showed that there were at least two different phases and no detectable $NaMnTe_2$. X-ray single-crystal structure determinations and elemental analyses (AA and WDS) showed that one of these phases was $Na_3Mn_4Te_6$.

$NaMn_{1.56}Te_2$ was first identified from the reaction product designed to synthesize $Na_3Mn_4Te_6$ at 850 °C. A mixture of Na, Mn, and Te in a 3:4:6 ratio was loaded into a Nb reaction vessel that was in turn sealed in an evacuated ($\sim 10^{-4}$ Torr) and flame-baked silica tube. The temperature of the reaction vessel was uniformly raised to 450 °C for 2 days, maintained at that temperature for 2 days, uniformly increased to 850 °C for 4 days, held at that temperature for 1 week, and finally cooled to room temperature at a rate of 2 °C/h. Powder diffraction data showed that there was a predominant unknown phase which has similar X-ray powder pattern as $NaMnTe_2$. Subsequent X-ray single-crystal structure determination and elemental analyses (AA and WDS) showed that this unknown phase was $NaMn_{1.56}Te_2$.

After we determined structures and compositions of $Na_3Mn_4Te_6$ and $NaMn_{1.56}Te_2$, we attempted to find the optimum reaction conditions for both compounds by changing reaction parameters such as temperature, loading conditions, heating and cooling speed, and reaction container. $Na_3Mn_4Te_6$ can be made by loading stoichiometric proportions of elemental starting materials in a Nb capsule. The temperature of the reaction vessel was uniformly raised to 450 °C for 2 days, maintained at that temperature for 2 days, uniformly increased to 600 °C for 2 days, held at that temperature for 1 week, and finally cooled to room temperature at a rate of 1 °C/h. Well-developed dark-red platelike crystals of $Na_3Mn_4Te_6$ were observed.

$NaMn_{1.56}Te_2$ can be synthesized directly: stoichiometric proportions of elemental starting materials were loaded into a Nb capsule, heated to 450 °C for 2 days, stayed at that temperature for 2 days, heated to 850 °C for 4 days, then stayed at 850 °C for 10 days, and slowly cooled to room temperature at a rate of 2 °C/h after reaction. The Guinier X-ray powder pattern shows that the major product was $NaMn_{1.56}Te_2$, a small amount of MnTe was also formed.

The synthesis of compounds $NaMn_xTe_2$ ($x = 1.5, 1.7, 2.0$) was attempted by mixing elemental starting materials, Na, Mn, and Te in stoichiometric proportions and heating at 850 °C for 200 h. Elemental analyses (WDS and AA) of products from each reaction container showed that the Mn composition ($x$) in each case was close to 1.56. Cell parameters for $NaMn_{1.56}Te_2$ determined for each sample were unchanged within experimental error. But MnTe and unidentified lines in the Guinier X-ray diffraction pattern indicated that the synthesis of pure $NaMn_{1.56}Te_2$ was elusive.

Incorporation of Te into the Nb containers to form binary compounds such as NbTe and $Nb_5Te_4$ was confirmed by WDS analyses on the inside wall of Nb tubes that were used in the synthesis of $NaMn_{1.56}Te_2$ at 850 °C. It seems likely that Nb−Te compound (NbTe and $Nb_5Te_4$) formation reduces the tellurium activity to an extent sufficient that manganese rich compounds such as $NaMn_{1.56}Te_2$ can be formed at higher reaction temperature (>750 °C). Preheating at 450 °C for 1 or 2 days reduces the reaction between Te and Nb container; presumably because Te activity is lowered by formation of binary tellurides such as $Na_2Te$ and MnTe.

To further explore the role of containers in these reactions, we conducted additional experiments using silica tubes for the synthesis of $NaMn_{1.56}Te_2$ and $Na_3Mn_4Te_6$. We could synthesize $NaMn_{1.56}Te_2$ and $Na_3Mn_4Te_6$ from loading stoichiometric proportions of starting materials ($Na_2Te$, Mn, and Te) in silica tubes which were evacuated and sealed. These silica tubes were heated to 450 °C for 2 days, kept at that temperature for 2 days, then heated to 600, 650, 750, and 850 °C at a rate of 10 °C/h in separate experiments, then held at each reaction temperature for 7 days, and slowly cooled to room temperature at a rate of 10 °C/h. Guinier X-ray diffraction patterns of the products of reactions designed to yield $NaMn_{1.56}Te_2$ showed that $NaMn_{1.56}Te_2$ was the predominant product, but the patterns exhibited unidentified lines as well. Unlike the situation when a Nb container was used, no MnTe was detected. Diffraction patterns observed when $Na_3Mn_4Te_6$ was the target product indicated the presence of mainly $Na_3Mn_4Te_6$, $MnTe_2$, and lesser amounts of unidentified phases. No MnTe and $NaMnTe_2$ were detected. This result contrasts with the results carried out in Nb container, in which no $MnTe_2$ was formed and $NaMn_{1.56}Te_2$ was formed at higher reaction temperature (>750 °C). A white reaction product stuck on inside of the silica tube after reaction probably results from a reaction between the silica tube and $Na_2Te$ to form ternary sodium silicate compounds, but we did not identify them.

From the results of these reactions, we could conclude that the formation of $NaMn_{1.56}Te_2$ is favored by loading stoichiometric amounts of starting materials in either Nb or silica tubes. $Na_3Mn_4Te_6$ can be synthesized at temperatures ranging from 600 to 850 °C in silica tubes by loading stoichiometric proportions of starting materials. We also observed that $Na_3Mn_4Te_6$ was formed at 600 °C by loading stoichiometric amounts of starting materials in a Nb container, but $NaMn_{1.56}Te_2$ forms instead at temperatures higher than 750 °C. Although silica tubes can be used for the synthesis of $Na_3Mn_4Te_6$ and $NaMn_{1.56}Te_2$, reaction products stick to the container walls and single crystals are not readily obtained.

$NaMnTe_2$ was not observed in several reaction attempts described above, but $Na_6MnTe_4$ was detected in reaction products when excess Na and Te (loading ratios of Na/Mn/Te were 3:1:4, 2:1:3, and 2:1:2) were used in reactions carried out from 600 to 850 °C in either Nb or silica tubes.

**Structure.** With the inclusion of larger alkali metal cations, $[MnTe_2]^-$ layers are formed by condensation of $MnTe_4$ tetrahedra at every vertex and Te atoms are arranged in tetragonal layers (square nets). Thus, the $AMnTe_2$ (A = K, Rb, Cs) compounds are isostructural with $TlFeS_2$.[26] The $[MnTe_2]^-$ layers in these compounds are essentially the same as layers found in red $HgI_2$,[27] though the layer stacking differs. A thermal ellipsoid plot of $KMnTe_2$ is shown in Figure 1. Selected bond distances and angles for $KMnTe_2$ and $RbMnTe_2$ are listed in Table 4. In this tetragonal structure, each layer is separated by alkali metals that center slightly compressed square prisms formed by 8 Te atoms. Distances to the surrounding Te atoms are 3.819(1) Å (× 8) for $KMnTe_2$ and 3.871(1) Å (× 8) for $RbMnTe_2$,

(27) Jeffrey, G. A.; Vlasse, M. *Inorg. Chem.* **1967**, *6*, 396−399.

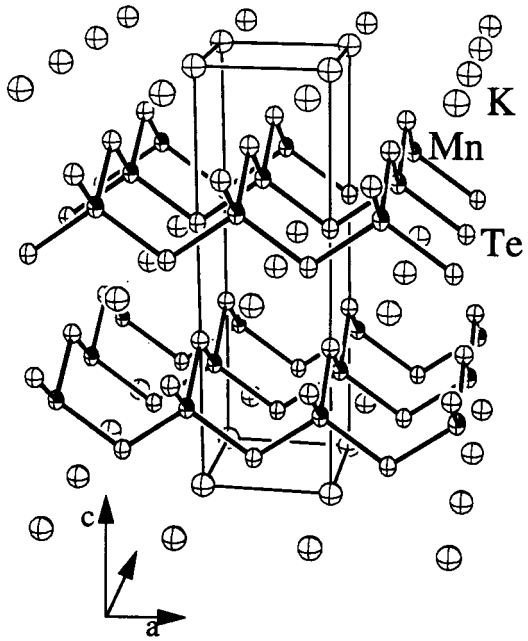


**Figure 1.** Thermal ellipsoid plot of $KMnTe_2$. 70% probability ellipsoids are shown.

**Table 4.** Selected Interatomic Distances (Å) and Angles (deg)

| | | | |
|---|---|---|---|
| | $KMnTe_2$ | | |
| Mn−Te (×4) | 2.782(1) | K−Te (×8) | 3.819(1) |
| Mn−Mn | 4.5110(4) | Te−Te | 4.5110(4) |
| Te−Mn−Te (×4) | 110.03(3) | Te−Mn−Te (×2) | 108.35(6) |
| Mn−Te−Mn | 108.35(6) | | |
| | $RbMnTe_2$ | | |
| Mn−Te (×4) | 2.777(1) | Rb−Te (×8) | 3.871(1) |
| Mn−Mn | 4.539(1) | Te−Te | 4.539(1) |
| Te−Mn−Te (×4) | 109.39(3) | Te−Mn−Te (×2) | 109.64(7) |
| Mn−Te−Mn | 109.64(7) | | |
| | $Na_3Mn_4Te_6$ | | |
| Mn−Te1 (×2) | 2.806(7) | Mn−Te2 | 2.770(6) |
| Mn−Te1 | 2.793(7) | Na2−Te2 (×2) | 3.113(4) |
| Na1−Te1 (×2) | 3.29(2) | Na1−Te1 (×2) | 3.560(4) |
| Na1−Te2 (×2) | 3.25(2) | Na2−Te1 (×4) | 3.397(3) |
| Mn−Te1−Mn | 72.8(2) | Mn−Te1−Mn | 75.1(2) |
| Mn−Te1−Mn | 117.0(2) | Mn−Te2−Mn | 113.6(3) |
| Te2−Mn−Te1 | 115.7(2) | Te2−Mn−Te1 | 107.9(2) |
| Te2−Mn−Te1 | 110.4(2) | Te1−Mn−Te1 | 106.8(2) |
| Te1−Mn−Te1 | 104.9(2) | Te1−Mn−Te1 | 111.1(2) |
| | $NaMn_{1.56}Te_2$ | | |
| Mn−Te (×3) | 2.749(3) | Te−Na (×6) | 3.255(2) |
| Mn−Te | 2.808(7) | Mn−Mn (×3) | 3.220(8) |
| Mn−Te−Mn (×3) | 109.8(2) | | |
| Mn−Te−Mn (×3) | 70.8(2) | | |
| Te−Mn−Te (×3) | 109.8(2) | | |
| Te−Mn−Te (×3) | 109.2(2) | | |

respectively. In contrast, Na atoms in $NaMnTe_2$ sit on trigonal antiprismatic sites surrounded by 6 Te atoms, a difference that is clearly attributable to the increased size of the heavier alkali metal cations. The $MnTe_4$ tetrahedra in $KMnTe_2$ and $RbMnTe_2$ are quite regular with Mn−Te distances of 2.782(2) Å (× 4) and 2.777(1) Å (× 4), respectively. The Te−Mn−Te angles are 108.35(6)° (× 2) and 110.03(3)° (× 4) in $KMnTe_2$ and 109.39(3)° (× 4) and 109.64(7)° (× 2) in $RbMnTe_2$. It is notable that $AMnTe_2$ (A = K, Rb, Cs) as well as $AMnTe_2$ (A = Li, Na) are the first compounds among the known ternary manganese tellurides that contain exclusively $Mn^{III}$.

The $Na_3Mn_4Te_6$ structure may be described as a hexagonal close-packed array of Te atoms with tetrahedral interstices

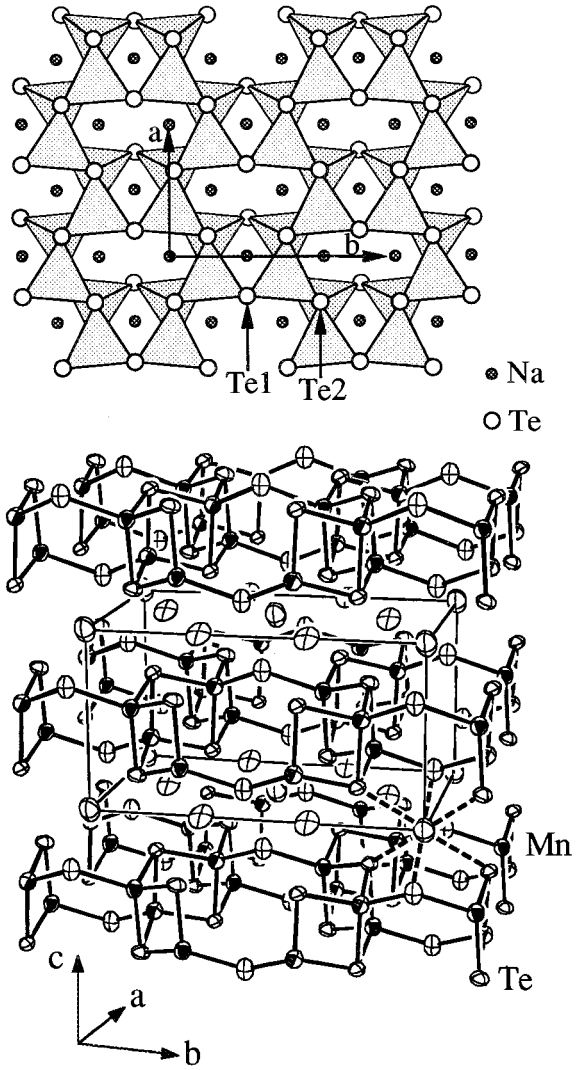


**Figure 2.** (Top) Polyhedral representation of two-dimensional $[Mn_4Te_6]^{3-}$ layer viewed on the *ab* plane. $MnTe_4$ tetrahedra are shown and Te atoms are shown as open circles, Na atoms as gray circles. (Bottom) Thermal ellipsoid (70% probability) plot of $Na_3Mn_4Te_6$ along the *c* axis. Na atoms within the unit cell are shown for clarity. The octahedral surroundings of one Na atom is with dashed lines.

filled with Mn atoms and octahedral interstices filled with Na atoms in a manner that generates a layered structure. A polyhedral representation of the $Na_3Mn_4Te_6$ layer viewed on the *ab* plane and a thermal ellipsoid plot projected approximately down the *a* axis are shown in Figure 2. Selected bond distances and angles for this compound are listed in Table 4. Mn atoms occupy tetrahedral sites between alternate Te layers into a pair of honeycomb (graphite-like) networks that comprise two-thirds of the tetrahedra that "point up" and two-thirds of tetrahedra that "point down". Consistent with this connectivity, each $MnTe_4$ tetrahedron shares Te vertexes with three adjacent tetrahedra in the same network. Within each $^2_\infty[Mn_4Te_6]^{3-}$ layer, the paired honeycomb nets are arranged so that each $MnTe_4$ tetrahedron shares two edges with tetrahedra in the other honeycomb net. The $MnTe_4$ tetrahedra are slightly distorted; Mn−Te bond distances in the tetrahedron fall into the range between 2.793(7) and 2.806(6) Å, and Te−Mn−Te angles are between 104.9(2) and 115.7(2)°. There are two crystallographically distinct Te atoms in the $Na_3Mn_4Te_6$; Te1 is bonded to two Mn atoms and Te2 is bonded to three ($^2_\infty[Mn_4Te_6] = {}^2_\infty[MnTe_{3/3}Te_{1/2}]$; Figure 2). There are two crystallographically

distinct Na atoms, all of which are coordinated to six Te atoms. Na atoms fill the octahedral interstices between $^{2}_{\infty}[Mn_4Te_6]$ layers. Na−Te bond distances range from 3.113(4) to 3.560(4) Å. $Na_3Mn_4Te_6$ is formally a $Mn^{III}/Mn^{II}$ mixed valence compound assuming all tellurium are $Te^{2-}$ (the shortest Te−Te contact is 4.495 Å).

XPS studies were attempted to determine whether the formal "mixed-valence" description we have used for Mn in $Na_3Mn_4Te_6$ might have some basis in observable properties. Unfortunately, we observed that the Mn $2p_{3/2}$ binding energy of $Na_3Mn_4Te_6$, 640.80 eV, was very close to the 640.67 eV found for $Mn^{III}$ in $NaMnTe_2$ and 640.87 eV for $Mn^{II}$ in MnTe. As a result, the investigation of Mn valency ($Mn^{II}$ vs $Mn^{III}$) in $Na_3Mn_4Te_6$ by comparison of Mn $2p_{3/2}$ binding energies was inconclusive. On the basis of the crystallographic equivalence of the all the Mn sites, we can only conclude that if there is mixed valency, no long-range order results from it.

The honeycomb net that is characteristic of the layers in $Na_3Mn_4Te_6$ is also observed a high-pressure form of $B_2O_3$.[28] Unlike the fusion of two nets in $Na_3Mn_4Te_6$, such nets in $B_2O_3$ are stacked up the *c* axis and linked together by fusion of corners. In Figure 2, it is clear that there are four empty tetrahedral sites within the unit cell. If these empty tetrahedral sites are filled up with Mn atoms, this would lead to the formula of the hypothetical compound, "$NaMn_2Te_2$", having all $Mn^{+1.5}$.

The crystal structure of $Na_3Mn_4Te_6$ can be traced back to a distorted close packed arrangement of Te atoms with hexagonal stacking sequence ABABAB, the stacking direction is perpendicular to *ab* plane. For an undistorted structure, the cell parameters should be related to those of a simple hcp unit cell ($a'$, $c'$) by

$$c' = c \sin \beta \quad (1)$$

$$a' = a/\sqrt{3} \quad (2)$$

$$a' = b/3 \quad (3)$$

The deviation of the actual structure from this idealized model is due to the fact that slightly different values for $a'$ are obtained from eqs 2 and 3; 4.777 and 4.694, respectively. The cell parameters obtained from the eqs 1−3 are similar to those of $NaMn_{1.56}Te_2$ and $NaMnTe_2$, and the axial ratio $c'/a'$ (1.59−1.62) is close to the ideal value 1.63 for simple hexagonal unit cell.

The structure of $NaMn_{1.56}Te_2$, projected approximately along the *c* axis, is shown in Figure 3. Selected bond distances and angles are listed in the Table 4. $NaMn_{1.56}Te_2$ is found to adopt a defective $CaAl_2Si_2$ structure type.[29] Again, fairly regular $MnTe_4$ tetrahedra are the building blocks of the structure having Mn−Te bond distances in the range of 2.749(3) to 2.808(7) Å and Te−Mn−Te angles 109.2(2) and 109.8(2)°. These tetrahedra share three edges in the formation of two-dimensional $[Mn_{1.56}Te_2]^-$ layers that are held together by ionic bonding to Na cations. There is one crystallographically unique Na atom in the structure which is coordinated to six Te atoms at a distance of 3.255(2) Å. Mn atoms partially occupy in the tetrahedral sites within layers and have an average formal charge of slightly less than +2. If these empty tetrahedral sites are filled up with Mn atoms, this again yields to the hypothetical compound, "$NaMn_2Te_2$".

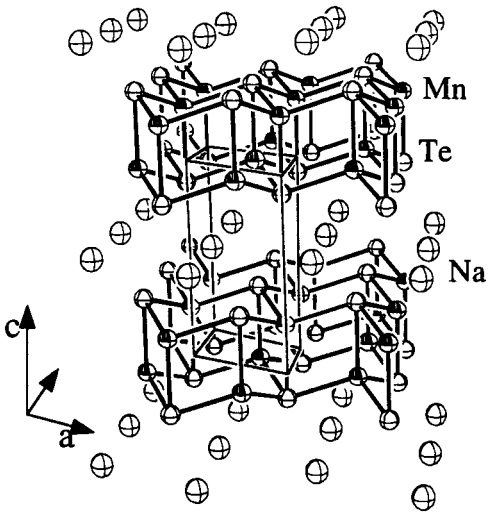


**Figure 3.** Thermal ellipsoid plot of $NaMn_{1.56}Te_2$. 70% probability thermal ellipsoids are shown.

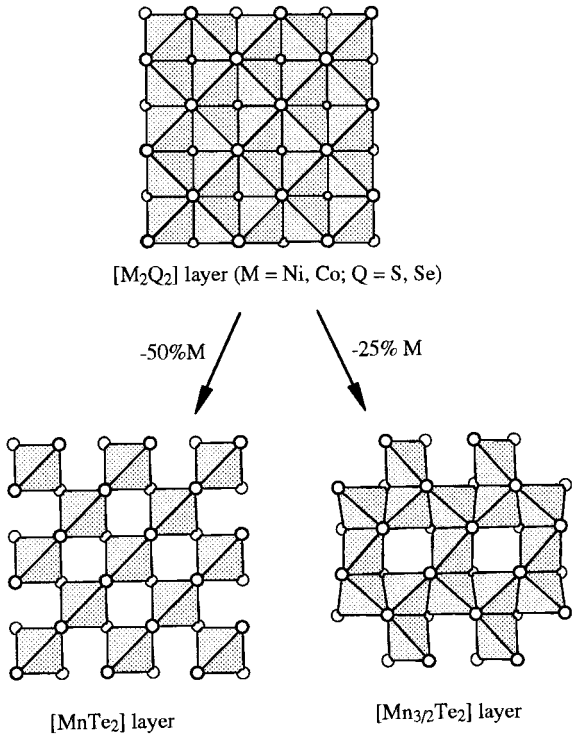


**Figure 4.** Structural relationships between $[M_2Q_2]$ in $AM_2Q_2$ (A = K, Rb, Cs; M = Ni, Co; Q = S, Se), $[Mn_{3/2}Te_2]$ (= $[Mn_3Te_4]$) in $A_2Mn_3Te_4$ where A = Rb, Cs, and $[MnTe_2]$ in $AMnTe_2$ (A = K, Rb, Cs). If one metal atom in every two is removed in $[M_2Q_2]$ layer, one obtains $[MnTe_2]$ layer. $[Mn_{3/2}Te_2]$ layer is formed if one metal atom is removed every four in a specific way.

**Structural Relationships.** There are close structural relationships between the title compounds and other compounds. The $TlFeS_2$ structure type adopted by the $AMnTe_2$ (A = K, Rb, Cs) compounds is closely related to $A_2Mn_3Te_4$ (A = Rb, Cs), and $AM_2Q_2$ (A = K, Rb, Cs; M = Ni, Co; Q = S, Se).[2,4] The manganese telluride layers in these compounds and their interrelationship are shown in Figure 4. Although "$AMn_2Te_2$" (A = alkali metal) with $ThCr_2Si_2$ structure type is not known, ternary cobalt and nickel selenides and sulfides with $ThCr_2Si_2$ structure type have been reported.[2] Ternary manganese silicides,

(28) Prewitt, C. T.; Shannon, R. D. *Acta Crystallogr.* **1968**, *B24*, 869−874.

(29) Gladyskevskii, E. I.; Kripajakevic, P. I.; Bodak, O. I. *Ukr. Fiz. Zh. (Russ. Ed.)* **1967**, *12*, 447.

(30) Siek, S.; Szytula, A.; Leciejewicz, L. *Phys. Stat. Sol.* **1978**, *46A*, K101−K105.

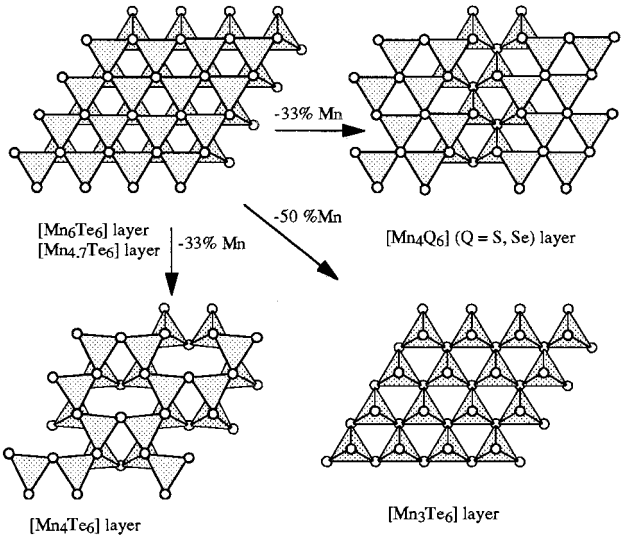


**Figure 5.** Structural relationships between the hypothetical compound "$NaMn_2Te_2$" (=$Na_3Mn_6Te_6$), and the real structures of $Na_3Mn_4Te_6$, $NaMn_{1.56}Te_2$ (=$Na_3Mn_{4.7}Q_6$), $Na_2Mn_2Q_3$ (=$Na_4Mn_4Q_6$; Q = S, Se), and $NaMnTe_2$ (=$Na_3Mn_3Te_6$). If approximately one-quarter of the Mn atoms are randomly removed from "$NaMn_2Te_2$", $NaMn_{1.56}Te_2$ is formed. If one-third of Mn atoms are removed from each Mn layer in two different ways, $Na_3Mn_4Te_6$ and $Na_2Mn_2Q_3$ (Q = S, Se) are obtained. If all Mn atoms from one layer removed, $NaMnTe_2$ is formed. Dark tetrahedra point up, pale gray down.

$RMn_2Si_2$ (R = Ce, Tb, Dy, Er, Th, Pr, Nd, Y), germanides, $RMn_2Ge_2$ (R = La, Ce, Pr, Nd, Sm, Y, Th), and a pnictide, $BaMn_2Sb_2$, with the $ThCr_2Si_2$ structure type are also known.[30−34]

The fundamental building blocks of these compounds are $MX_4$ (X = S, Se, Si, Ge, Sb) tetrahedra. In the $AM_2Q_2$ (A = K, Rb, Cs; M = Ni, Co; Q = S, Se) type, each transition metal atom is tetrahedrally coordinated to chalcogen, and in turn each chalcogen is bonded to 4 metal atoms. Consequently, four edges of the $MQ_4$ tetrahedra are shared with adjacent tetrahedra to form a 2-dimensional layer, $^2_\infty[Mn_{4/4}Q_{4/4}]^-$. The alkali metal atom is located in the center of a compressed cube formed by 8 chalcogen atoms. If every second Mn atom is removed, one obtains $^2_\infty[Mn_{4/4}Te_{4/2}]^-$ layers in $AMnTe_2$ (A = K, Rb, Cs). As a result, metal−metal contacts observed in of $AM_2Q_2$ (A = K, Rb, Cs; M = Ni, Co; Q = S, Se), are comparatively short and range between 2.634 and 2.761 Å, while the shortest Mn−Mn distances in $AMnTe_2$ (A = K, Rb, Cs) range between 4.511 (3) and 4.569 (1) Å. This difference may be responsible for the metallic character of $AM_2Q_2$ (A = K, Rb, Cs; M = Ni, Co; Q = S, Se).[2] $A_2Mn_3Te_4$ (A = Rb, Cs) structures are obtained if one Mn atom in every four is removed in a specific way to form another layer, $^2_\infty[MnTe_{4/3}]^{3-}$.[4] Mn−Mn contacts in these compounds range from 3.269(1) to 3.346(4) Å.

We can also compare $Na_3Mn_4Te_6$, $NaMn_{1.56}Te_2$, $AMnTe_2$ (A = Li, Na), and $Na_2Mn_2Q_3$ (Q = S, Se).[35,36] Relationships between these compounds are illustrated in Figure 5. As was also mentioned above, a complete filling of the tetrahedral sites with Mn atoms in $Na_3Mn_4Te_6$ and $NaMn_{1.56}Te_2$ results in the formation of hypothetical compound with composition "$NaMn_2Te_2$" ($CaAl_2Si_2$ structure type). This can also be viewed as parent compound of $AMnTe_2$ (A = Li, Na). This type of structure is observed in the ternary silver sulfide, $BaAg_2S_2$ [37] and ternary manganese pnictides, $AMn_2Pn_2$ (A = Ca, Sr, Ba, Pn = P, As; A = Ca, Sr, Pn = Sb).[34,38,39] Each layer in "$NaMn_2Te_2$" has a [Te−Mn−Mn−Te] stacking sequence. If approximately one-quarter of the Mn atoms are randomly removed from the [$Mn_2Te_2$] layer, $NaMn_{1.56}Te_2$ (≡$Na_3Mn_{4.7}Te_6$) results. The layer in $Na_3Mn_4Te_6$ can be obtained from those in "$NaMn_2Te_2$" by removing $^1/_3$ of the Mn atoms ($\sqrt{3} \times \sqrt{3}$ superlattice) from the two hexagonal sheets within such layers ([$Mn_{4/3}Te_2$] = [Te−$Mn_{2/3}$−$Mn_{2/3}$−Te]). In $Na_2Mn_2Q_3$ (Q = S, Se), $^1/_3$ of the Mn atoms are removed with a different ordering (zigzag).[35,36]

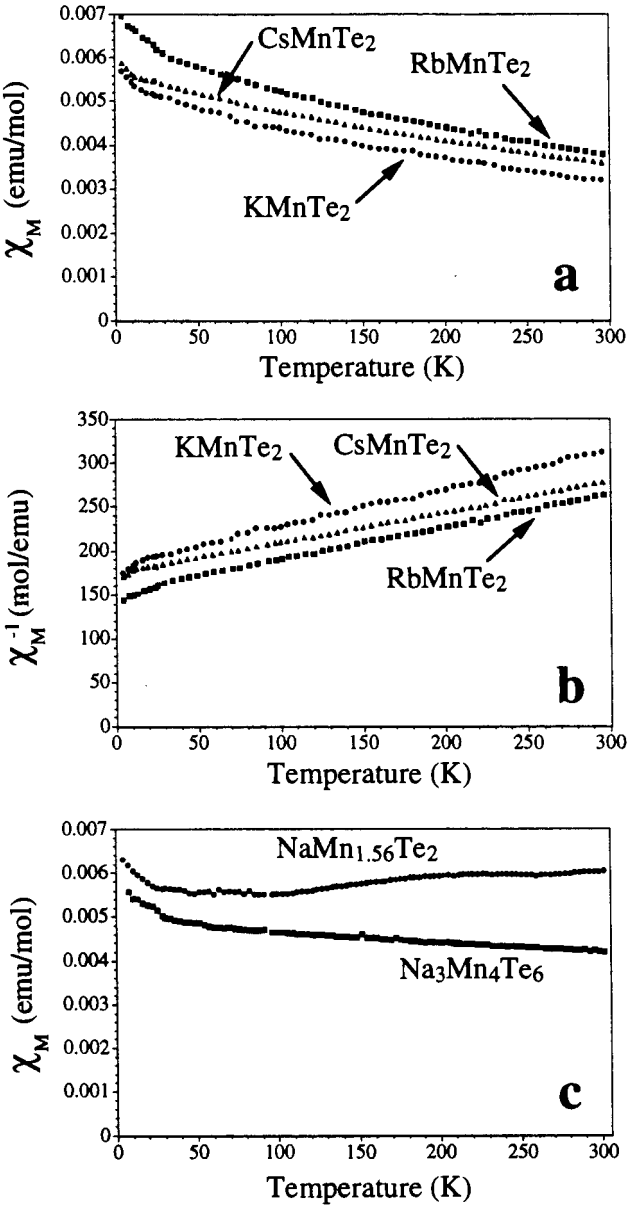


**Figure 6.** (a) Observed molar magnetic susceptibilities of $AMnTe_2$ (A = K, Rb, Cs). (b) Inverse susceptibilities of $AMnTe_2$ (A = K, Rb, Cs). (c) Observed molar magnetic susceptibilities of $NaMn_{1.56}Te_6$ and $Na_3Mn_4Te_6$.

(31) Siek, S.; Szytula, A.; Leciejewicz, J. *Solid State Commun.* **1981**, *39*, 863−866.
(32) Ban, Z.; Omejec, L.; Szytula, A.; Tomkowicz, Z. *Phys. Stat. Sol.* **1975**, *27A*, 333−339.
(33) Szytula, A.; Szott, I. *Solid State Commun.* **1981**, *40*, 199−202.
(34) Brechtel, E.; Cordier, G.; Schäfer, H. *Z. Naturforsch* **1978**, *33B*, 820−822.
(35) Klepp, K.; Böttcher, P.; Bronger, W. *J. Solid State Chem.* **1983**, *47*, 301−306.
(36) Kim, J.; Hughbanks, T. Unpublished results.
(37) Bronger, W.; Lenders, B.; Huster, J. *Z. Anorg. Allg. Chem.* **1997**, *623*, 1357−1360.
(38) Cordier, G.; Schäfer, H. *Z. Naturforsch* **1976**, *31b*, 1459−1461.
(39) Mewis, A. *Z. Naturforsch* **1978**, *33B*, 606−609.

Finally, if all atoms from one Mn layer are removed, one obtains the polar [$MnTe_2$] layer which we recently reported.[19]

The size of alkali metal cations plays a key role in structural transition from $CaAl_2Si_2$ type to $ThCr_2Si_2$ type in a series of compounds $AMnTe_2$ (A = Li, Na, K, Rb, Cs). Larger alkali metal cations destabilize the "$NaMn_2Te_2$" ($CaAl_2Si_2$ structure type) in favor of $ThCr_2Si_2$ type structure. This trend is also evident in a series of compounds $CaMn_2As_2$, $SrMn_2As_2$, and $BaMn_2As_2$;[34] the former two compounds adopt $CaAl_2Si_2$ structure type, whereas the last one adopts the $ThCr_2Si_2$ type structure.

**Magnetic Measurements.** The temperature-dependent molar magnetic susceptibilities for $AMnTe_2$ (A = K, Rb, Cs) are shown in Figure 6a and b. The reciprocal magnetic susceptibilities of these compounds show nearly linear temperature variation. For $T > 40$ K, these data were fit to a modified Curie−Weiss expression ($\chi = \chi_0 + N\mu_{eff}^2/(T - \theta)$, where $\chi_0$ accounts for temperature-independent contributions, $\theta$ is the Weiss constant, $\mu_{eff}$ is the effective magnetic moment per Mn center, and $N$ and $k_B$ are Avogadro's and Boltzmann's constants). The following parameters were obtained: for $KMnTe_2$, $\chi_0 = 2.53 \times 10^{-5}$ emu/mol, $\theta \cong -420$ K, and $\mu_{eff} = 4.31\ \mu_B$; for $RbMnTe_2$, $\chi_0 = 2.38 \times 10^{-5}$ emu/mol, $\theta \cong -420$ K, and $\mu_{eff} = 4.71\ \mu_B$; for $CsMnTe_2$, $\chi_0 = 7.26 \times 10^{-5}$ emu/mol, $\theta \cong -510$ K, and $\mu_{eff} = 4.86\ \mu_B$. The effective magnetic moments are in reasonable agreement with the value of 4.90 $\mu_B$ ($S = 2$) expected for a free high-spin $Mn^{III}$ ion in a tetrahedral field. The large negative values of the Weiss constants for each of these compounds probably indicate strong antiferromagnetic interactions between localized $Mn^{III}$ ions. This result is consistent with other 2-dimensional ternary manganese selenides with tetragonal arrangements of Mn ions, e.g., $A_2Mn_3Se_4$ (A = Rb, Cs).[4] Neutron diffraction studies for these ternary selenide examples revealed that the Mn spins were antiferromagetically arranged within layers. The low-temperature upturns in our measured magnetic susceptibilities might be due to the presence of paramagnetic impurities which were not detectable by X-ray diffraction analysis.

Temperature-dependent magnetic susceptibilities for $NaMn_{1.56}Te_2$ and $Na_3Mn_4Te_6$ over the temperature range 4−300 K are plotted in Figure 6c. Magnetic susceptibilities of both compounds exhibit nearly temperature-independent paramagnetism over the temperature range 30−300 K. The magnetic susceptibility of $Na_3Mn_4Te_6$ decreases slightly from 0.00497 emu/mol at 30 K to 0.00421 emu/mol at 300 K, whereas the magnetic susceptibility of $NaMn_{1.56}Te_2$ increases slightly from 0.00565 emu/mol at 30 K to 0.00604 emu/mol at 300 K. The magnitude of these compounds' room-temperature susceptibilities are comparable to those measured for the $A^IMnTe_2$ (A = K, Rb, Cs) compounds, but the deviation from Curie Law behavior suggests even stronger interaction between moments.

**Concluding Remarks.** The layered compounds, $AMnTe_2$ (A = K, Rb, Cs), $Na_3Mn_4Te_6$, and $NaMn_{1.56}Te_2$, have been synthesized and characterized by the use of single-crystal and powder X-ray diffraction, microprobe analysis, atomic absorption spectroscopy, and temperature-dependent magnetic studies. The proper choice of reaction condition parameters such as temperature and cooling speed, reaction vessels, starting materials, and their stoichiometry are important for successful syntheses. Close structural relationships are observed between title compounds and other compounds which are already known. All title compounds form layered structures with the $MnTe_4$ tetrahedron as the fundamental building block. All compounds have different formal oxidation states, $Mn^{III}$ in $AMnTe_2$ (A = K, Rb, Cs), $Mn^{2.25+}$ in $Na_3Mn_4Te_6$, and $Mn^{II}$ in $NaMn_{1.56}Te_2$. Temperature-dependent magnetic susceptibilities measurements show that $AMnTe_2$ (A = K, Rb, Cs) exhibit Curie−Weiss paramagnetism, whereas $Na_3Mn_4Te_6$ and $NaMn_{1.56}Te_2$ show paramagnetism with a weak dependence on temperature.

**Acknowledgment.** This research was generously supported by the Texas Advanced Research Program through Grant 010366-097 and National Science Foundation through Grant DMR-9215890. The R3m/V single-crystal X-ray diffractometer and crystallographic computing system were purchased from funds provided by the National Science Foundation (Grant CHE-8513273). We thank Dr. Renald Guillemette, Dr. Anatoly Bortun, and Mr. Aaron Dumar for their assistance with the microprobe analyses, atomic absorption measurements, and magnetic susceptibilities measurements.

**Supporting Information Available:** Tables of anisotropic displacement parameters for $KMnTe_2$, $RbMnTe_2$, $Na_3Mn_4Te_6$, and $NaMn_{1.56}Te_2$ (1 page). Ordering information is given on any current masthead page.

IC980805W